Available online at www.sciencedirect.com

ScienceDirect

Procedia Computer Science 218 (2023) 24–34

Procedia Computer Science

www.elsevier.com/locate/procedia

International Conference on Machine Learning and Data Engineering

Classification of Breast Thermal Images into Healthy/Cancer Group Using Pre-Trained Deep Learning Schemes

Seifedine Kadry[a], Rubén González Crespo[b], Enrique Herrera-Viedma[c], Sujatha Krishnamoorthy[d,e,*], and Venkatesan Rajinikanth[f]

[a]*Faculty of Applied Computing and Technology, Noroff University College, Kristiansand, 94612, Norway*
[b]*Computer Science Department, School of Engineering and Technology, Universidad Internacional de La Rioja, 26006, Spain* [b]*Andalusian*
[c]*Research Institute in Data Science and Computational Intelligence, University of Granada, Granada, Spain*
[d]*Zhejiang Bioinformatics International Science and Technology Cooperation Center, Wenzhou-Kean University, Zhejiang Province, China,*
[e]*Wenzhou Municipal Key Lab of Applied Biomedical and Biopharmaceutical Informatics, Wenzhou-Kean University, Zhejiang Province, China.*
[f]*Department of Computer Science and Engineering, Saveetha School of Engineering, SIMATS, Chennai 602105, Tamil Nadu, India*

Abstract

In the women's community, Breast Cancer (BC) is a severe disease. The World Health Organization reported in 2020 that 2.26 million deaths occur due to BC. BC is curable if detected early. Since thermal imaging is non-invasive and supports disease detection, it is commonly used in clinics. Compared to other methods, it keeps BC early and accurate. The proposed work aims to evaluate the performance of the Pretrained Deep-Learning Methods (PDLM) in detecting BC using the thermal images collected from the benchmark dataset. It includes the following stages: primary image processing, deep feature mining, handcrafted feature mining, feature optimization using Firefly-Algorithm (FA), classification and validation. Visual Lab thermal images were used in the study. The investigational outcome of this study authenticates that the VGG16, along with the DT, provides better detection accuracy (95.5%) compared to other classifiers used in this study. To justify the significance of the implemented technique, the proposed work not only improved accuracy, but also improved precision, sensitivity, specificity, and F1-Scores.

Keywords: Breast cancer; Thermal imaging; Firefly algorithm; Feature optimization; Classification.

1. Introduction

Recently, cancer in internal/external organs has emerged as severe disease in humankind, and timely discovery and handling are essential. The former findings in the literature substantiate that premature discovery will facilitate

* Corresponding author. Tel.: +86 133 3691 3765
E-mail address: Sujathaks@ieee.org

10.1016/j.procs.2022.12.398

curing cancer with suitable treatment. Cancer in organs is caused chiefly due to irregular and unrestricted cell growth [1-3].

The year 2020 report of WHO specifies that cancer is the prime reason for 10 million deaths internationally. This statement also substantiates that cancer in the following organs reason for the foremost sickness globally; (i) Breast, (ii) Lung, (iii) Colon, (iv) Prostate, (v) Skin, and (vi) Stomach. Among these cancers, it is established that the BC incidence speed is significant (2.26 million cases), and it caused a reported death of 685 000 individuals [4].

Because of its occurrence rate and the death pace, several screening measures are planned to notice BC in its early phase. The standard methods followed in cancer diagnosis occupy; an individual check to notice the abnormality/lump in the breast region, biomedical-imaging supported diagnosis, and needle biopsy supported BC severity verification. When the distinct phase of the cancer is recognized, proper treatment procedures, such as medicine, chemotherapy, and operation, are executed to heal the illness [5,6].

A biomedical-imaging-based examination is one of the extensively approved screening methodologies for BC recognition, and the imaging trials, such as Magnetic-Resonance-Imaging, Ultrasound, and Thermal-Imaging (TI), are extensively employed. TI is one of the newly adopted non-invasive procedures and helps detect BC in its early phase. The earlier works related to TI-based BC detection confirm that this method helps distinguish the premature and the sensitive form of cancer with better accuracy. Further, the imaging system is simple, and it needs only a particular camera (thermal camera) that records the thermal radiation of the skin surface. The TI can be examined in gray-scale and RGB-scale form, and the analysis of this image involves detecting the change in thermal pattern. This image helps detect Ductal Carcinoma In Situ (DCIS) and the low/high-grade BC.

This research aims to execute the DLM-supported assessment system to categorize the pre-processed thermal images into healthy/cancer classes. This work's investigation confirms that the VGG16 scheme with Decision-Tree-Classifier (DTC) helps achieve better detection accuracy (95.5%).

The contribution of this study contains;

i. Execution of different deep-learning methods to categorize test imagery into healthy/cancer set
ii. Implementing Firefly-algorithm based feature selection methodology to advance the cancer detection accuracy.

As for the other divisions of this report, Section 2 will show the earlier research, Section 3 will present the methodology, and Sections 4 and 5 will present the results and conclusions.

2. Related Research

BC occur in women due to different grounds, such as fatness, contact to radiation, alcohol utilization, genetics, age, and delayed pregnancy. Along with these causes, different other inferior reasons also initiated the probabilities of the BC. Earlier research confirms that the precise recognition of the BC with suitable imaging methodology helps in appropriate treatment. Every picture presents the probable answer to detect the BC for treatment preparation and execution. A summary of the BC detection procedures found in the literature is presented in Table 1:

Table 1. Summary of breast cancer detection using medical imaging scheme

Reference	Implemented assessment technique
Kadry et al. [7]	The thresholding and segmentation integration is implemented to mine the tumour in breast MRI. The thresholding procedure will enhance the essential section in the image and then enhances the information, which is then mined and analysed with chosen segmentation scheme.
Elanthirayan et al. [8]	Heuristic algorithm based joint thresholding and segmentation is implemented to mine the tumor in breast MRI. This scheme executes a united threshing and segmentation technique.
Thanaraj et al. [9]	Extraction of the BC region in the ultrasound image is discussed using Shannon's entropy and level-set scheme.
Vijayakumar et al. [10]	Machine-learning (ML) supported classification of benign/malignant breast cancer is

	presented using ultrasound image.
Nair et al. [11]	Identification of BC with image processing system is presented and the product confirms the superiority of combined thresholding and segmentation
Rajinikanth et al. [12]	Automatic categorization of TI into normal/cancer class is presented using the ML scheme.
Dey et al. [13]	ML supported classification of breast TI into early/acute DCIS class is presented in this work using binary classifiers.

Table 1 authenticates that the imaging-based analysis of the BC is standard and suitable discovery is necessary to cure the illness in its early stage. In this work, the TI-based discovery of the BC is presented using the DLM, and the results are discussed. Compared to the other DLM, the VGG16 presents superior detection accuracy. Further, this system helps in accurate detection, which is essential when a low-power analytic procedure is employed.

3. Methodology

This division of the research presents the outline planned to examine the BC using the TI, and this scheme is shown in Figure 1. Various tasks implemented in this proposal are as follows; (i) Initial check by the individual (patient) to verify the abnormal lump in the breast, (ii) Clinical level screening of the BC using the TI, (iii) Examination of the breast section in various angle orientations (angle, $\theta = 0^o$,$\theta = 45^o$,$\theta = -45^o$, $\theta = 90^o$ and $\theta = -90^o$) to screen the whole breast section, (iv) Image pre-processing to convert the raw TI into a usable form, (v) Resizing and feature extraction using the suitable method and (vi) Feature selection, classification, and validation. In this work, the necessary features from the TI are mined using the DLM and the chosen traditional methods, like LBP and PHOG. Later, FA-based feature reduction is employed to find the optimal HF and avoid the over-fitting issue.

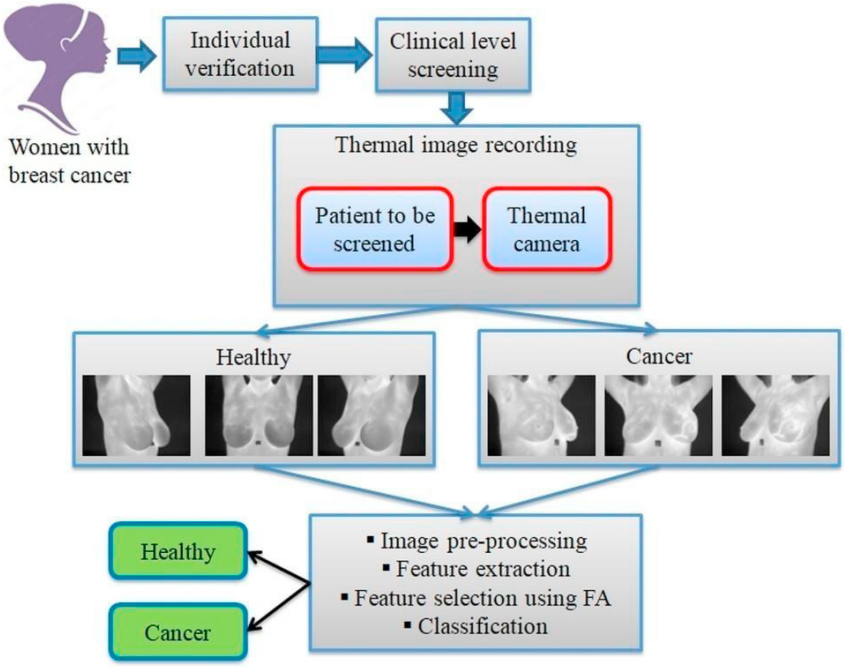

Fig 1. Automatic detection of BC using the TI

This work evaluates the performance of the DF-based classification for AlexNet, VGG16, VGG19, ResNet8, and ResNet50 using the SM classifier. When the best DLM is determined, a 50% dropout is used to reduce the DF value, and these features are then serially concatenated with the HF to form a hybrid feature vector. The developed framework's performance is verified again using this feature vector. In this process, the performance of the classification process is verified using SM, DT, RF, KNN, and SVM classifiers. The outcome of this process confirms that the VGG16 helps provide a better BC detection compared to other classifiers and the DT offers superior classification accuracy.

3.1. Breast thermal image

The TI supported BC screening utilize a thermal-camera to collect the necessary breast image data based on the recommended clinical protocol [14-17]. Throughout this task the breast TI is registered at different orientations to get the complete information about the breast section and the sample images collected from the database for healthy/cancer class images are shown in Figure 2. Fig 2(a) to (e) shows the breast section with different angle orientations. From this image, the left and the right breast sections are then extracted for the analysis as in Figure 3. Fig 3(a) shows the cropped breast section, Fig 3(b) presents the right breast and Fig 3(c) shows the left breast section. These images are then resized based on the chosen DLM and the resized images are then considered to extract the features. Table 2 shows the total number of images including the TI considered for training, testing and validation.

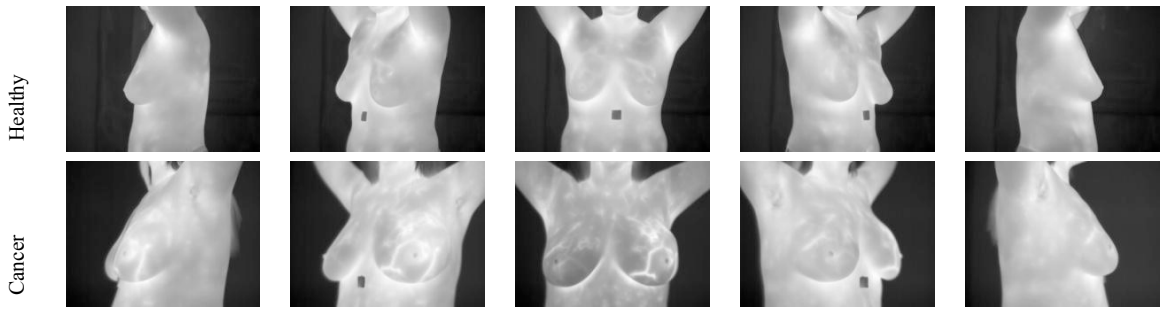

(a) $\theta = 90^o$ (b) $\theta = 45^o$ (c) $\theta = 0^o$ (d) $\theta = 45^o$ (e) $\theta = 90^o$

Fig 2. Breast sections recorded at different orientation

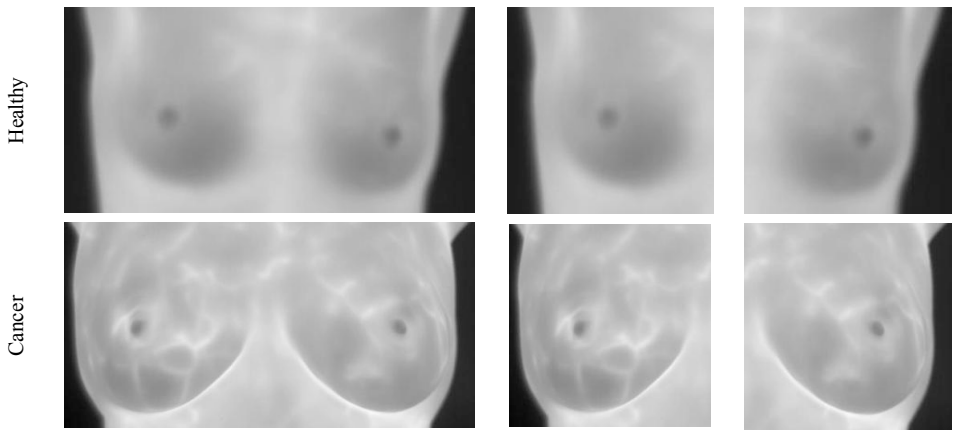

(a) Region of interest (b) Left (c) Right

Fig 3. Sample breast sections considered for the examination

Table 2. The test images considered to evaluate the developed BC detection framework

Class	Dimension	Total	Training (70%)	Testing (20%)	Validation (10%)
Normal	$224\times 224\times 3$	1000	700	200	100
Abnormal	$224\times 224\times 3$	1000	700	200	100

3.2. Pre-trained Deep Learning Methods

The present research works performed using the medical images confirms that DLM based disease detection provides a better detection accuracy compared to other traditional schemes. Pre-trained schemes such as AlexNet, VGG16, VGG19, ResNet18 and ResNet50 are widely used in the literature for analyzing medical images due to their accuracy. This work considers the PDL schemes, hence the initial parameters are assigned follows based on the literature; Initial weights= ImageNet, Batch value=8, Epochs=100, Optimizer=Adam, Pooling=Maximum, Monitoring metric= Accuracy and Loss, Classifier=SoftMax with a 5-fold cross-validation [18-20].

3.3. Feature extraction and Reduction

This research work considers two types of features from the test images; (i) DF mined with DLM and (ii) HF obtained with LBP and PHOG. The extracted DF from each DLM is of dimension $1\times1\times1000$ and this is considered to classify the TI using the SM initially. After verifying the performance of this scheme, then the classification task is repeated using serially combined DF and HF and the achieved results are then verified. During this process, the DF is reduced to half with the help of 50% dropout and the optimal HF are obtained using the FA based feature selection. These procedures are depicted in this section with appropriate mathematical expressions. Eqn. (1) presents the actual DF obtained from DLM and Eqn. (2) shows the DF after 50% dropout. In this work, the DF of VGG16 is considered, since it offered a betted accuracy on the considered TI dataset.

$$DF_{1\,(1\times1\times1000)} = DF_{(1,1)}, DF_{(1,2)}, \ldots, DF_{(1,1000)} \tag{1}$$

$$DF_{2\,(1\times1\times500)} = DF_{(1,1)}, DF_{(1,2)}, \ldots, DF_{(1,500)} \tag{2}$$

The necessary handcrafted features are obtained with LBP and PHOG and the necessary information on these features are depicted in Figure 4 and 5 correspondingly. The necessary information on these features can be found in [21]. The LBP features are collected using the varied weight values of W= 1 to 4 and the PHOG features are collected using various bins of B= 1 to 3. The HF associated with LBP and PHOG are depicted in Eqns. (3) and (4). Eqn. (5) presents the HF which is the combined values of Eqn. (3) and (4). This equation value is then optimized with the FA and the optimized value is then serially combined with the DF depictedin Eqn. (2).

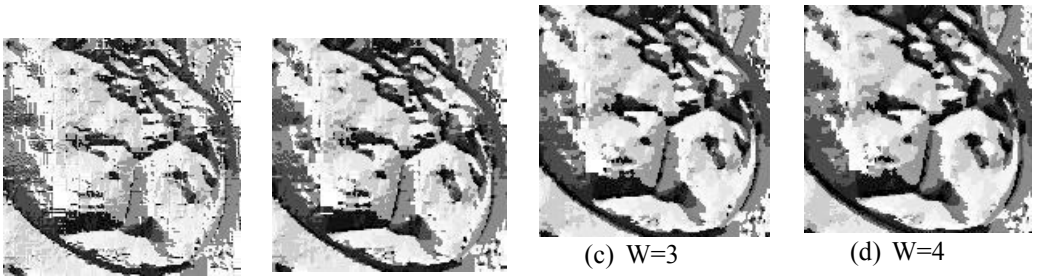

(c) W=3 (d) W=4

Fig 4. LBP feature obtained for a sample image for W= 1 to 4

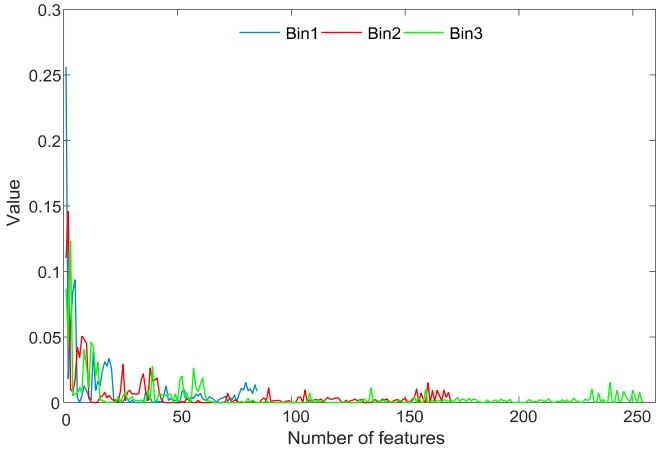

Fig 5. PHOG feature obtained for a sample image for B= 1 to 3

$$LBP_{(1\times1\times236)} = LBP_{1\,(1\times1\times59)} + LBP_{2\,(1\times1\times59)} + LBP_{3\,(1\times1\times59)} + LBP_{4\,(1\times1\times59)} \quad (3)$$

$$PHOG_{(1\times1\times510)} = PHOG_{1\,(1\times1\times85)} + PHOG_{2\,(1\times1\times170)} + PHOG_{3\,(1\times1\times255)} \quad (4)$$

$$HF_{(1\times1\times746)} = LBP_{(1\times1\times236)} + PHOG_{(1\times1\times510)} \quad (5)$$

In machine-learning and deep-learning scheme, the feature reduction is widely engaged to reduce the attribute vector dimension to evade the over-fitting issue. Heuristic algorithm based attribute reduction is a common methodology and this work employs FA based scheme is implemented to fined features. The complete information regarding the FA based feature optimization is discussed in [22] and this work adopts the procedure to reduce the HF vector.

The concept of the feature reduction is simple and in this work, the Cartesian Distance (CD) between the fireflies is considered to find the best features. The complete information about this scheme can be found in the earlier works. In this research, the FA strictures are allocated as follows; Fly value= 30, Total iterations= 2000, the performance measure= maximal CD and terminating criteria= maximal iteration or maximal CD. The implemented FA helps to reduce the feature vector as present in Eqn. (6) and the combined DF and HF (DF+HF) is depicted in Eqn. (7). Eqn. (7) is then considered to verify the performance of the developed framework using various binary classifiers and to justify the performance, a 5-fold cross-validation is considered.

$$HF_{1\,(1\times1\times284)} = LBP_{(1\times1\times115)} + PHOG_{(1\times1\times169)} \quad (6)$$

$$DF + HF_{(1\times1\times784)} = DF_{(1\times1\times500)} + HF_{1\,(1\times1\times284)} \quad (7)$$

3.4. Performance evaluation

Performance metric computation and verification of the performance is a necessary scheme in automatic disease detection procedure. The merit of proposed framework depends on the features and the classifiers. In this research, the classifiers, such as SM, DT, RF, KNN and SVM with linear kernal is implemented. The necessary metrics, like AC, PR, SE, SP, and FS, are calculated and based on these metrics, the benefit of poposed scheme is verified. The mathematical appearance these metrica are depicted in Eqns. (8) to (12);

$$AC = \frac{TP + TN}{TP + TN + FP + FN} \quad (8)$$

$$PR = \frac{TP}{TP + FP} \quad (9)$$

$$SE = \frac{TP}{TP + FN} \tag{10}$$

$$SP = \frac{TN}{TN + FP} \tag{11}$$

$$FS = \frac{2TP}{2TP + FN + FP} \tag{12}$$

4. Experimental Results and Discussions

This section of research displays the investigational results. This experimental is executed with a computed having an Intel i7 processor, 20GB RAM, and 4GB VRAM equipped with Python®.

The considered TI dataset is initially examined using the chosen DLM with DF alone, and the BC detection accuracy is verified using the SM classifier. The attained result with every DLM is presented in Table 3 and this result substantiate the outcome of VGG16 is superior. The overall performance of VGG16 is then assessed using the Glyph-plot as in Figure 6 verifies the performance of VGG16.

Table 3. Performance metric achieved with SM classifier

Scheme	TP	FN	TN	FP	AC	PR	SE	SP	FS
AlexNet	91	9	88	12	89.5000	88.3495	91.0000	88.0000	89.6552
VGG16	94	5	92	9	93.0000	91.2621	94.9495	91.0891	93.0693
VGG19	92	8	90	10	91.0000	90.1961	92.0000	90.0000	91.0891
ResNet18	90	11	91	8	90.5000	91.8367	89.1089	91.9192	90.4523
ResNet50	92	8	92	8	92.0000	92.0000	92.0000	92.0000	92.0000

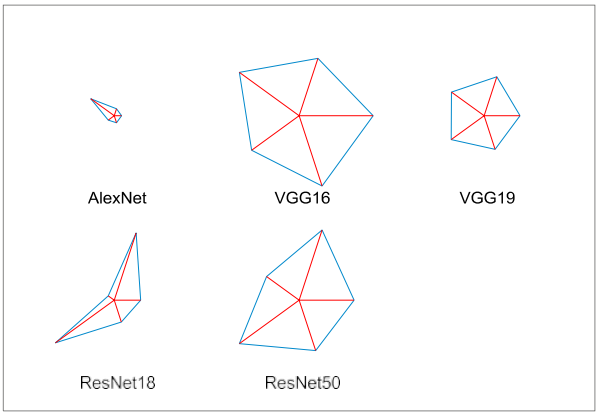

Fig 6. Glyph-plot of Table 3 metrics

The DF obtained from VGG16 is then considered for further examination, and to reduce its feature, a 50% dropout is applied. This feature is combined with the FA-selected deep feature to get a new feature vector, as shown in Eqn. (5). Figure 7 shows the different convolutional stage results for a chosen test image. Fig 7(a) shows the test image, and Fig 7(b) to (e) presents the results achieved from the convolutional layer 1 to 4 (Conv1 to 4), respectively. Figure 8 presents the experimental outcome achieved for DF+HF with the DT classifier. Fig 8(a) and (b) show the accuracy and loss values, and Fig 8(c) presents the CM with the necessary values of TP, FN, TN, and FP values. Figure 8(d) shows the ROC curve with an achieved AUC of 0.966. This

classification provided a BC detection accuracy of 95.5%, and other related values and similar classification results of considered classifiers are presented in Table 4.

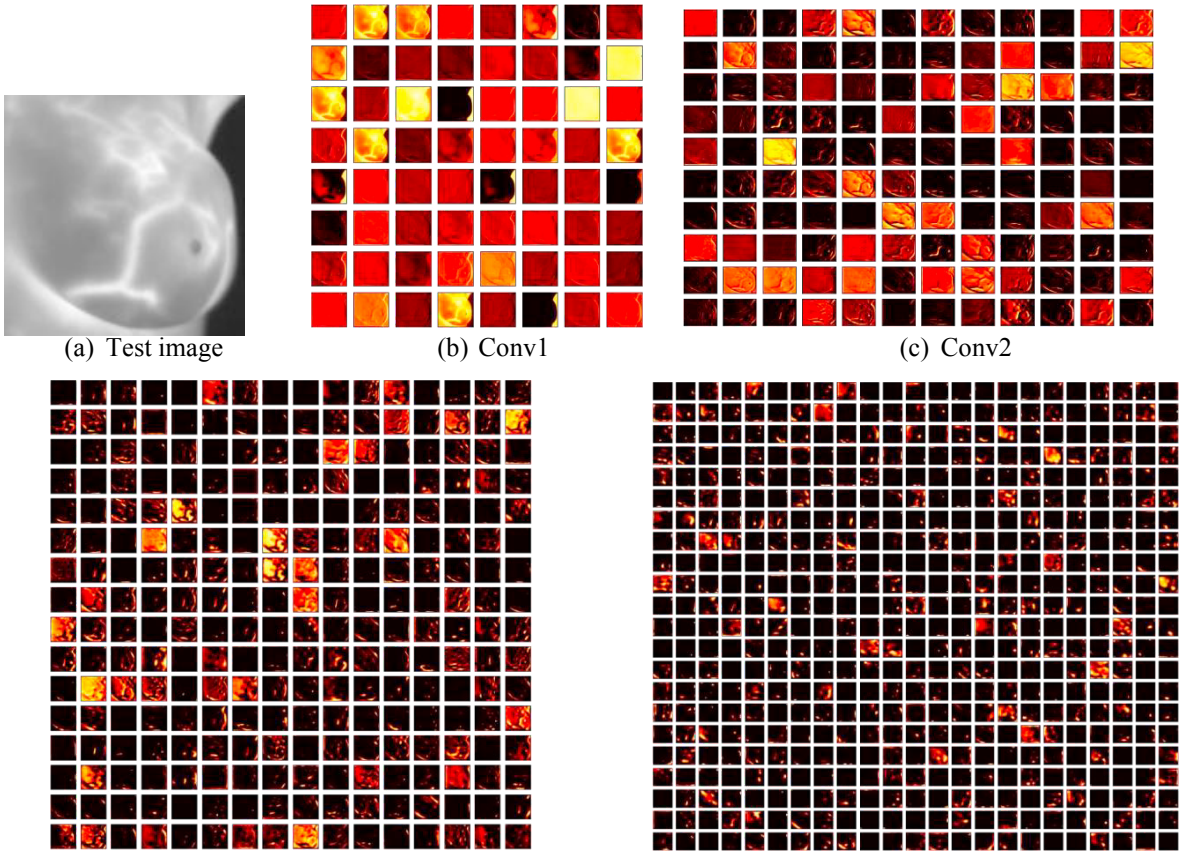

(a) Test image (b) Conv1 (c) Conv2

(d) Conv1 (e) Conv4

Fig 7. Various convoolutional layer outcome of VGG16 for a chosen test image

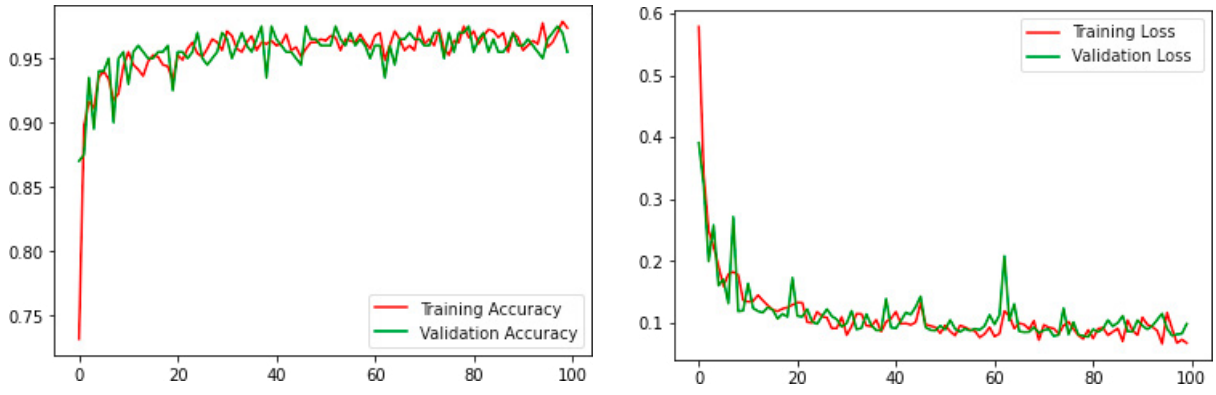

(a) Accuracy (b) Loss

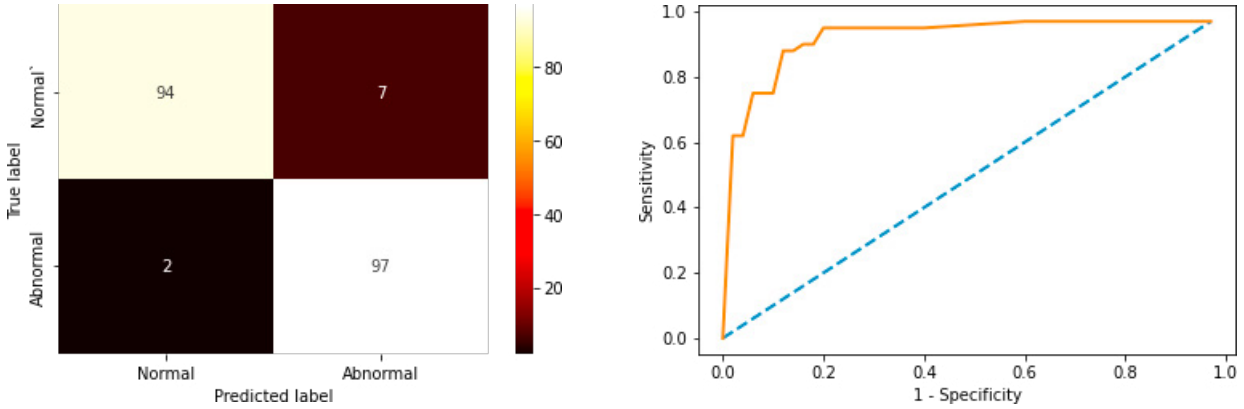

(c) Confusion matrix (d) RoC curve

Fig 8 Experimental result achieved for DF+HF with DT classifier

Table 4. Performance metric for RF+HF and DT classifier

Scheme	TP	FN	TN	FP	AC	PR	SE	SP	FS
SM	95	5	94	6	94.5000	94.0594	95.0000	94.0000	94.5274
DT	97	2	94	7	95.5000	93.2692	97.9798	93.0693	95.5665
RF	95	5	95	5	95.0000	95.0000	95.0000	95.0000	95.0000
KNN	94	6	95	5	94.5000	94.9495	94.0000	95.0000	94.4724
SVM	93	7	95	5	94.0000	94.8980	93.0000	95.0000	93.9394

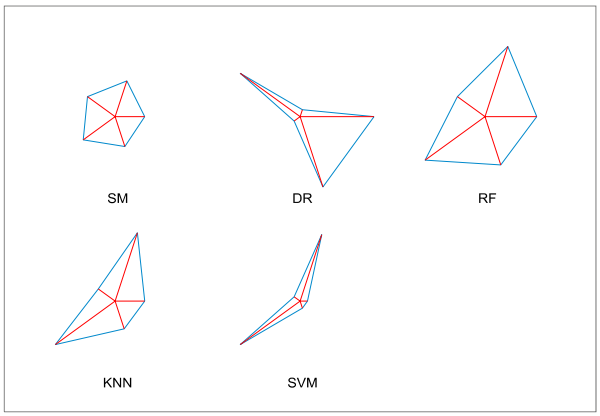

Fig 9. Glyph-plot to confirm the merit of his proposed classifiers

Figure 9 presents the overall merit of implemented scheme and the DT-based disease classification. This image confirms that the DT classifier provides better accuracy; hence, in the future, this framework will help detect the BC using the TI collected from the hospitals.

5. Conclusions

This section presents the experimental outcome using various classifiers and the merit of a chosen technique is verified. This research aim to distinguish the cancer in TI with betted accuracy to plan and execute the treatment.

This research implements a DLM-supported BC detection using the TI. The detection is performed with DF and DF+HF separately and the achieved results are compared. The investigational work of this scheme confirms that the result reached with VGG16 is healthier. The outcome of the DT is then compared and verified with other binary classifiers. This scheme helps to achieve a detection accuracy of 95.5% using the DF+HF and the result of this study confirms that this scheme is better. The experimental outcome confirms the excellence of this technique on the benchmark database.

Nomenclature

BC	breast cancer
BTI	breast thermal image
CM	confusion matrix
CNN	convolutional neural network
DF	deep features
DLM	deep learning method
DT	decision tree
FA	firefly algorithm
FN	false-negative
FP	false-positive
KNN	K-nearest neighbours
PHOG	pyramid histogram of oriented gradients
RF	random forest
SM	SoftMax
TI	thermal imaging
TN	true-negative
TP	true-positive
WHO	world health organisation

References

[1] Jain, D., Singh, V., 2018. Diagnosis of breast cancer and diabetes using hybrid feature selection method. In 2018 Fifth International Conference on Parallel, Distributed and Grid Computing (PDGC), IEEE, 64-69. DOI: 10.1109/PDGC.2018.8745830

[2] Singh, V., Asari, V. K., Rajasekaran, R., 2022. A deep neural network for early detection and prediction of chronic kidney disease. Diagnostics, 12(1): 116.

[3] Jung, A. Y., Ahearn, T. U., Behrens, S., Middha, P., Bolla, M. K., Wang, Q., ... CTS Consortium., 2022. Distinct reproductive risk profiles for intrinsic-like breast cancer subtypes: pooled analysis of population-based studies. JNCI: Journal of the National Cancer Institute.

[4] https://www.who.int/news-room/fact-sheets/detail/cancer

[5] Huo, Y., Yu, J., Gao, S., 2022. Magnetic-mediated hyperthermia for cancer treatment: Research progress and clinical trials. Synthesis and biomedical applications of magnetic nanomaterials, 228-260.

[6] Matthews, H. K., Bertoli, C., de Bruin, R. A., 2022. Cell cycle control in cancer. Nature Reviews Molecular Cell Biology, 23(1), 74-88.a

[7] Kadry, S., Damaševičius, R., Taniar, D., Rajinikanth, V., Lawal, I. A.: 2021. Extraction of tumour in breast MRI using joint thresholding and segmentation–A study. In 2021 Seventh International conference on Bio Signals, Images, and Instrumentation (ICBSII) (pp. 1-5). IEEE (2021, March). DOI: 10.1109/ICBSII51839.2021.9445152

[8] Elanthirayan, R., Sakeenathul Kubra, K., Rajinikanth, V., Sri Madhava Raja, N., Satapathy, S. C., 2021. Extraction of Cancer Section from 2D Breast MRI Slice Using Brain Strom Optimization. In Intelligent Data Engineering and Analytics (pp. 731-739). Springer, Singapore, 731-739. https://doi.org/10.1007/978-981-15-5679-1_71

[9] Ifan Roy Thanaraj, R., Anand, B., Allen Rahul, J., Rajinikanth, V., 2020. Appraisal of breast ultrasound image using Shannon's thresholding and level-set segmentation. In Progress in Computing, Analytics and Networking, Springer, Singapore, 621-630. https://doi.org/10.1007/978-981-15-2414-1_62

[10] Vijayakumar, K., Rajinikanth, V., Kirubakaran, M. K., 2022. Automatic detection of breast cancer in ultrasound images using Mayfly algorithm optimized handcrafted features. Journal of X-Ray Science and Technology, (Preprint), 1-16. DOI: 10.3233/XST-221136

[11] Nair, M. V., Gnanaprakasam, C. N., Rakshana, R., Keerthana, N., Rajinikanth, V., 2018. Investigation of breast melanoma using hybrid image-processing-tool. In 2018 International Conference on Recent Trends in Advance Computing (ICRTAC), IEEE, 174-179. DOI: 10.1109/ICRTAC.2018.8679193

[12] Rajinikanth, V., Kadry, S., Taniar, D., Damaševičius, R., Rauf, H. T., 2021. Breast-cancer detection using thermal images with marine-predators-algorithm selected features. In 2021 Seventh International conference on Bio Signals, Images, and Instrumentation (ICBSII), 1-6. DOI: 10.1109/ICBSII51839.2021.9445166

[13] Dey, N., Rajinikanth, V., Hassanien, A. E., 2021. An examination system to classify the breast thermal images into early/acute DCIS class. In Proceedings of International Conference on Data Science and Applications, Springer, Singapore, 209-220. https://doi.org/10.1007/978-981-15-7561-7_17

[14] Rajinikanth, V., Raja, N. S. M., Satapathy, S. C., Dey, N., Devadhas, G. G., 2017. Thermogram assisted detection and analysis of ductal carcinoma in situ (DCIS). In 2017 International Conference on Intelligent Computing, Instrumentation and Control Technologies (ICICICT), IEEE, 1641-1646 . DOI: 10.1109/ICICICT1.2017.8342817

[15] https://visual.ic.uff.br/dmi/

[16] Borchartt, T. B., Resmini, R., Motta, L. S., Clua, E. W., Conci, A., Viana, M. J., ... Sanchez, A., 2012. Combining approaches for early diagnosis of breast diseases using thermal imaging. International Journal of Innovative Computing and Applications 17, 4(3-4), 163-183.

[17] Joshi, B., Sharma, A. K., Yadav, N. S., Tiwari, S., 2021. DNN based approach to classify Covid'19 using convolutional neural network and transfer learning. International Journal of Computers and Applications, 1-13.

[18] Sharif, M. I., Li, J. P., Khan, M. A., Kadry, S., Tariq, U., 2022. M3BTCNet: multi model brain tumor classification using metaheuristic deep neural network features optimization. Neural Computing and Applications, 1-16.

[19] Zhang, L., Li, C., Peng, D., Yi, X., He, S., Liu, F., ... Huang, X., 2022. Raman spectroscopy and machine learning for the classification of breast cancers. Spectrochimica Acta Part A: Molecular and Biomolecular Spectroscopy, 264, 120300.

[20] Jasti, V., Zamani, A. S., Arumugam, K., Naved, M., Pallathadka, H., Sammy, F., ... Kaliyaperumal, K., 2022. Computational technique based on machine learning and image processing for medical image analysis of breast cancer diagnosis. Security and Communication Networks.

[21] Khan, M. A., Rajinikanth, V., Satapathy, S. C., Taniar, D., Mohanty, J. R., Tariq, U., Damaševičius, R., 2021. VGG19 network assisted joint segmentation and classification of lung nodules in CT images. Diagnostics, 11(12), 2208.

[22] Sawhney, R., Mathur, P., Shankar, R., 2018. A firefly algorithm based wrapper-penalty feature selection method for cancer diagnosis. In International Conference on Computational Science and Its Applications, Springer, Cham, 438-449.